

Electrical and chemical characterization of the Schottky barrier formed between clean n-GaN(0001) surfaces and Pt, Au, and Ag

Cite as: Journal of Applied Physics **94**, 3939 (2003); <https://doi.org/10.1063/1.1598630>

Submitted: 28 March 2003 • Accepted: 12 June 2003 • Published Online: 29 August 2003

K. M. Tracy, P. J. Hartlieb, S. Einfeldt, et al.



View Online



Export Citation

ARTICLES YOU MAY BE INTERESTED IN

[High barrier height GaN Schottky diodes: Pt/GaN and Pd/GaN](#)

Applied Physics Letters **68**, 1267 (1996); <https://doi.org/10.1063/1.115948>

[The physics and chemistry of the Schottky barrier height](#)

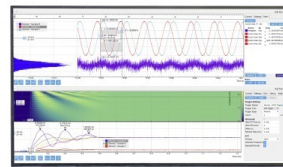
Applied Physics Reviews **1**, 011304 (2014); <https://doi.org/10.1063/1.4858400>

[Schottky barrier on n-type GaN grown by hydride vapor phase epitaxy](#)

Applied Physics Letters **63**, 2676 (1993); <https://doi.org/10.1063/1.110417>

Challenge us.

What are your needs for periodic signal detection?



Zurich
Instruments

Electrical and chemical characterization of the Schottky barrier formed between clean *n*-GaN(0001) surfaces and Pt, Au, and Ag

K. M. Tracy, P. J. Hartlieb, ^{a)} S. Einfeldt, and R. F. Davis

Department of Materials Science and Engineering, North Carolina State University, Raleigh, North Carolina 27695-7907

E. H. Hurt and R. J. Nemanich

Department of Physics, North Carolina State University, Raleigh, North Carolina 27695-8202

(Received 28 March 2003; accepted 12 June 2003)

Platinum, gold, and silver formed abrupt, unreacted, smooth, and epitaxial metal–semiconductor interfaces when deposited from the vapor onto clean, *n*-type GaN(0001) films. The Schottky barrier heights, determined from data acquired using x-ray photoelectron spectroscopy, ultraviolet photoelectron spectroscopy, capacitance–voltage, and current–voltage measurements agreed to within the experimental error for each contact metal and had the values of 1.2 ± 0.1 , 0.9 ± 0.1 , and 0.6 ± 0.1 eV for Pt, Au, and Ag, respectively. The band bending and the electron affinity at the clean *n*-GaN surface were 0.3 ± 0.1 and 3.1 ± 0.1 eV, respectively. The barrier height is proportional to the metal work function, indicating that the Fermi level is not pinned at the GaN surface. However, discrepancies to the Schottky–Mott model were found as evidenced by a proportionality factor of 0.44 between the work function of the metal and the resulting Schottky barrier height. The sum of these discrepancies constitute the interface dipole contributions to the Schottky barrier height which were measured to be ~ 1.4 , 1.3, and 0.7 eV for Pt, Au, and Ag, respectively. © 2003 American Institute of Physics. [DOI: 10.1063/1.1598630]

I. INTRODUCTION

GaN-based compounds are being extensively investigated for applications in blue and ultraviolet emitting optoelectronic and high-frequency microelectronic devices. The achievement of *p*-type GaN has allowed the development of blue and green light emitting diodes (LEDs), blue emitting laser diodes, and nitride-based heterojunction bipolar transistors.^{1–4} GaN-based metal–semiconductor field effect transistors (MESFET)^{5–7} and metal–semiconductor–metal photodetectors (MSM)^{8–10} have also been realized. The development of thermally stable rectifying contacts with large breakdown voltages and low leakage currents are particularly important for the MESFET and MSM device structures. The future improvement of each of these devices rests in part on a detailed understanding of the metal/semiconductor interface of the rectifying contact.

Numerous studies have investigated Pt,^{11–20,29} Au,^{12,13,20–30,33,34} and Ag^{13,31–34} rectifying contacts on the *n*-GaN(0001) surface. The large work function of these metals as well as the fact that they form abrupt, unreacted metal–semiconductor interfaces that are reported to be thermally stable to 600 °C³⁵ makes them excellent candidates for MESFET devices. The realization of ideal Schottky contacts for the aforementioned device applications depends in large part on the properties of the underlying semiconductor surface. As such, *n*-GaN films are often prepared using an *ex situ* pretreatment that is intended to remove native O and C contamination at the semiconductor surface that would preclude the formation of an intimate metal–semiconductor

contact. However, all of the *ex situ* techniques investigated to date, including dilute HCl,^{12,13,19,33,34} boiling aqua-regia [HCl:HNO₃(3:1)],^{16,23,26} buffered oxide etch,^{17,18,32} and KOH,^{22,29} result in an incomplete removal of the aforementioned contaminants. Contacts subsequently deposited on these contaminated surfaces result in Schottky barrier heights that are dependent on the applied bias. As this is in sharp contrast to the ideal behavior described by thermionic emission theory, the ideality factors reported for these contaminated contact structures are routinely much larger than 1. It has also been suggested³⁶ that the interfacial contamination is responsible for the disagreement between the Schottky barrier heights measured using current–voltage (*I*–*V*) and capacitance–voltage (*C*–*V*) techniques.

As all of the *ex situ* cleaning methods noted above result in only a partial removal of the native O and C contamination, it is reasonable to assume that significant nonuniformities are produced in the remaining contamination across the *n*-GaN surface. Metal contacts subsequently deposited over these nonuniform areas would result in isolated regions of the interface with a low Schottky barrier height, as the removal of surface contamination results in a local reduction of the barrier height. It has been suggested³⁷ that these nonuniformities in the Schottky barrier height would also be manifest in ideality factors in excess of 1.

In situ surface preparation methods, including ultrahigh vacuum (UHV) annealing,²⁹ Ga metal deposition and desorption,^{31,32,38} and multiple cycles of N-ion sputtering followed by UHV annealing (ISA)²⁰ have been explored in an attempt to overcome the deficiencies of the *ex situ* methods outlined above. Wu *et al.*²⁰ showed that ISA procedures are

^{a)}Electronic mail: pjhartl@clemsun.edu

TABLE I. Summary of reported experimental studies of Schottky contacts on *n*-GaIn.

| Contact | Contact diameter(μm) | Ionized charge (cm^{-5}) | <i>ex situ</i> treatment | <i>in situ</i> treatment | $\Phi_b I - V$ (eV) | $\Phi_b C - V$ (eV) | Φ_b XPS (eV) | Ideality factor <i>n</i> | Leakage at -10 V (A) | Reference |
|---------|-----------------------------------|-------------------------------------|--|--------------------------|---------------------|---------------------|-------------------|--------------------------|-------------------------|-----------|
| Pt | NR | NR | NR | ISA | NR | NR | 1.65 | NR | NR | 20 |
| Pt | NR | NR | NR | NR | NR | NR | NR | NR | NR | 1 |
| Pt | 250 | 1×10^{17} a | O ₂ descum, dilute HCl, H ₂ O | NR | 1.01–1.08 | 1.16 | NR | 1.05 | 5×10^{-6} | 12 |
| Pt | NR | 3×10^{17} b | NR | NR | 1.11 | 1.1 | NR | 1.7 | NR | 14 |
| Pt | 75 | 2×10^{17} a | O ₂ plasma, NH ₄ OH:H ₂ O(1:10), H ₂ O | NR | 1.11 | 1.1 | NR | 1.7 | NR | 15 |
| Pt | 75 | NR | boiling aquaregia, organic solvents, alcohol | NR | 1.1 | 1.106 | NR | 1.002–1.05 | 1×10^{-9} | 16 |
| Pt | 100, 200, 400 | 9.4×10^{16} a | BOE:H ₂ O(1:10) | NR | 1.13 | 1.27 | NR | 1.1 | NR | 17 |
| Pt | 100, 200, 400 | 1.2×10^{17} a | BOE:H ₂ O(1:10) | NR | 0.89 | 1.12 | NR | 1.05 | NR | 17 |
| Pt | 80, 160, 320, 640 | 2×10^{17} a | BOE | NR | 1.03 | 1.04 | NR | 1.21 | $\sim 1 \times 10^{-6}$ | 18 |
| Pt | 320 | NR | organics, HCl:H ₂ O | NR | 0.88 | 1 | NR | 1.32 | NR | 19 |
| Au | 250 | 1×10^{17} a | O ₂ descum, dilute HCl, H ₂ O rinse | NR | 0.86–0.88 | 0.98 | NR | 1.04 | 1×10^{-7} | 12 |
| Au | NR | 6×10^{17} b | NR | NR | 1.03 | 1.03 | NR | 1.15 | NR | 22 |
| Au | NR | 6×10^{17} b | KOH:H ₂ O, boiling H ₂ O | NR | 1.03 | 1.03 | NR | 1.15 | NR | 21 |
| Au | 217 | 6.6×10^{16} b | boiling aquaregia, organic solvents, alcohol | NR | 0.844 | 0.94 | NR | 1.03 | 1×10^{-10} | 23 |
| Au | 300 | NR | NH ₄ OH:H ₂ O(1:10), H ₂ O | NR | 0.8 | 1.02 | NR | 1.14 | NR | 24 |
| Au | 217 | 6.6×10^{16} b | NR | NR | 0.91 | 1.01 | NR | 1.04 | 1×10^{-9} | 25 |
| Au | 400 | 7×10^{17} a | boiling aquaregia vapor, isopropyl alcohol | NR | 0.98 | 1.16 | NR | 1.4 | NR | 26 |
| Au | NR | NR | NR | NR | 1.19 | 1.15 | NR | NR | NR | 27 |
| Au | NR | 2×10^{16} a | organics, HF:H ₂ O(1:10), H ₂ O | NR | 0.8–1.1 | NR | NR | 1.6–4 | 2×10^{-5} | 28 |
| Au | NR | NR | NR | ISA | NR | NR | 1.3 | NR | NR | 20 |
| Au | 150 | 2.45×10^{16} b | HCl, H ₂ O | NR | 0.91 | 1.05 | NR | 1.46 | NR | 33 |
| Au | NR | 1.2×10^{17} a | hot KOH and aqua-regia | UHV annealing 900 °C | NR | NR | 1.15 | NR | NR | 29 |
| Au | ~ 1000 | NR | TCE, acetone, methanol, isopropanol, (HCl:DI) | NR | 1.08–1.88 | NR | NR | 1.21–1.56 | NR | 30 |
| Ag | 250 | 1×10^{17} a | O ₂ plasma asher, dilute HCl | NR | 0.54 | 0.66 | NR | 1.24 | $\sim 1 \times 10^{-3}$ | 13 |
| Ag | 170 | 6×10^{16} a | HF:H ₂ O(1:10), H ₂ O | Ga dep. and desorption | 0.77 | NR | 0.7 ± 0.2 | 1.6 | NR | 31 |
| Ag | 1000 | NR | HF:NH ₄ F:NH ₄ OH | Ga dep. and desorption | 0.7 | NR | NR | 1.57 | NR | 32 |
| Ag | 150 | 2.45×10^{16} b | HCl, H ₂ O | NR | 0.89 | 1.61 | NR | 1.34 | NR | 33 |

NR=not reported.

a)Hall measurement.

b)=CV measurement.

ISA=Nion sputter and anneal.

UHV=ultrahigh vacuum.

TCE=trichloroethylene.

effective for obtaining clean and ordered *n*-type GaN surfaces. In this case a large portion of the damage induced by N-ion sputtering was subsequently recovered by high-temperature annealing. The Schottky barriers of Pt and Au contacts deposited on ISA-prepared *n*-GaN surfaces were calculated from the results of x-ray photoelectron spectroscopy (XPS) spectra to be 1.65 and 1.3 eV, respectively.

Kampen *et al.*³² measured the Schottky barrier of Ag and Pb contacts on *n*-GaN surfaces prepared using an *ex situ* treatment in HF:NH₄F:NH₄OH in conjunction with a Ga deposition and desorption technique. A previous study³⁹ by the same authors suggests that this surface preparation method results in clean and ordered surfaces with upward band bending of approximately 0.4 eV. *I*-*V* measurements revealed barrier heights of 0.82 and 0.73 eV and ideality factors (*n*) of 1.57 and 1.28 for the Ag and the Pb contacts, respectively. In this case the large ideality factors persisted even though the native surface contamination was apparently removed. Similar to the study by Wu *et al.*,²⁰ the absence of additional independent measurements of the barrier height makes it difficult to identify the source of the nonideal behavior. The contact structures, experimental conditions, and corresponding barrier heights from previously reported studies of Pt, Au, and Ag Schottky contacts on *n*-type GaN are summarized in Table I.

The following sections detail the results and conclusions of a comprehensive study of the chemical and electrical properties of Pt, Au, and Ag Schottky contacts deposited on *n*-type GaN(0001) films which have been pretreated using an NH₃-based, high temperature chemical vapor clean (CVC). XPS and ultraviolet photoelectron spectroscopy (UPS) were employed to evaluate the chemical and electrical properties of the *n*-GaN surface in the pretreated and metallized states. The Schottky barrier heights were measured *in situ* and were subsequently compared to *ex situ* measurements that were made on the same contact structures using *I*-*V* and *C*-*V* techniques. The use of a combination of four independent characterization methods provided a unique opportunity to study the details regarding Schottky barrier formation on clean and ordered *n*-GaN surfaces.

A companion article concerned with the electrical, structural, mechanical, and microstructural characteristics of the as-deposited and annealed interfaces of the Pt(111)/GaN(0001) and Au(111)/GaN(0001) assemblies investigated in the present research has been published.³⁵ It was determined that the growth mode of the Pt and Au thin films followed the two-dimensional Frank-van der Merwe model. Both of the as-deposited metal films were abrupt, unreacted, monocrystalline, and epitaxial with a (111)/(0001) relationship with the GaN. The rectifying behavior of both contacts degraded after annealing at 400 °C for 3 min; they became ohmic after annealing at 600 °C (Au) or 800 °C (Pt) for the same time.

II. EXPERIMENT

The 1.1 μm thick, Si-doped GaN thin films used in this study were grown via organometallic vapor phase epitaxy on a 0.1 μm thick AlN buffer layer previously deposited at 1150

°C on Si-terminated, on-axis 6H-SiC(0001) substrates. The wurtzite films were oriented in the [0001] direction and were presumed to be Ga terminated.^{40,41} *C*-*V* measurements acquired using a Hewlett Packard 4284A *C*-*V* measurement system and a MDC mercury probe station indicated a net impurity concentration ($N_D - N_A$) of $1 \times 10^{17} \text{ cm}^{-3}$.

Tungsten was subsequently sputtered onto the backside of the SiC substrates to assist in radiative heating of the transparent samples throughout the *in situ* preparation process. Prior to loading, the films were cleaned sequentially in trichloroethylene (TCE), acetone, and methanol ultrasonic baths for 10 min each, followed by a 10 min dip in 49% hydrochloric acid and a 10 s rinse in deionized (DI) water. The details of the effects of this cleaning process have been published elsewhere.⁴¹ The samples were fastened to a molybdenum plate and subsequently attached to a molybdenum sample holder, which facilitated the transfer process throughout the experiment. There was an approximate 10 min interval between extracting the sample from the DI rinse and loading it into an integrated surface analysis and growth system operating at a base pressure of $(1 \pm 2) \times 10^{-9}$ Torr and equipped with XPS, UPS, low-energy electron diffraction (LEED), electron beam metallization, and chemical vapor cleaning facilities.

An ammonia-based high temperature chemical vapor process⁴¹ was used to obtain clean, stoichiometric *n*-type GaN surfaces. To achieve these surfaces, the sample was initially heated to 500 ± 10 °C, whereupon the ammonia flux was introduced. The sample was then heated to 860 ± 25 °C and held for 15 min at a process pressure of $(9 \pm 1) \times 10^{-5}$ Torr. As the distance between the ammonia doser and the sample was ~5 cm, the partial pressure of ammonia at the sample surface may have been as much as an order of magnitude greater than the system pressure. Upon cooling to 200 ± 10 °C the sample was immediately transferred in ultra-high vacuum (UHV) for photoelectron spectroscopy measurements and subsequent metallization. The surface temperature was monitored throughout the process with an Ircon infrared pyrometer at an emissivity setting of 0.5. Temperatures outside the operating range of the pyrometer (<600 °C) were determined using the thermocouple mounted immediately behind the sample.

XPS measurements were made using a Fisons XR3 dual anode x-ray source coupled to a Fisons CLAM II hemispherical electron energy analyzer with a mean radius of 100 mm operating at a base pressure of 2×10^{-10} Torr. The resolution of the analyzer was 1.0 eV, although the absolute peak positions could be measured to within 0.1 eV. All core level spectra were fit using a nonlinear "S" type Shirley background^{42,43} and a mixed Gaussian-Lorentzian peak type. UPS measurements were made using an Omicron HIS13 gas discharge lamp together with a RHK 500 mm mean radius hemispherical electron energy analyzer. A negative 4 Volt bias was applied to the sample throughout the measurement to overcome the work function of the spectrometer. The analyzer was operated with a resolution of approximately 0.1 eV. All spectra were acquired at an operating pressure of $(7 \pm 3) \times 10^{-9}$ Torr while the base pressure of the system was $< 3 \times 10^{-10}$ Torr. The Fermi level position was

determined from UPS measurements made on clean Ni films.

Pt (99.999%), Au (99.9999%), or Ag (99.999%) were deposited onto the GaN(0001) surface at room temperature using an electron-beam evaporation system with a base pressure of 2×10^{-10} Torr before and less than 6×10^{-9} Torr during deposition. Typical deposition rates were 0.09 – 0.12 nm/s. Prior to deposition onto the sample surface, approximately 5 nm of metal was evaporated while a shutter covered the sample surface to remove contamination that might have accumulated on the source metal surface. The thickness of the deposited metal layers was increased stepwise from 0.02 nm to a maximum of 75 nm. The thickest films of 70 – 75 nm were used to approximate a “bulk” layer of the respective metals.

Following the completion of the aforementioned *in situ* experiments, the samples were removed from vacuum and patterned using photolithography. First, 100 μm diameter Schottky contact pads were formed using positive photoresist and etched in aqua-regia (3:1:1 HCl: HNO₃: H₂O) at 85 °C for 10 s, in aqua-regia at room temperature for 5 s, and in nitric acid at room temperature for 5 s for Pt, Au, and Ag, respectively. The samples were then placed in a deionized water bath for 30 s and rinsed in acetone and methanol for 1 min each to remove the photoresist. Second, 100 μm wide ohmic contact rings surrounding the pads were formed using negative photoresist, thermal evaporation of Al (99.999%), and a metal lift-off process. The *I*–*V* characterization was performed using a Keithley 236 source measure unit. *C*–*V* curves were recorded under reverse bias at a frequency of 1 MHz using a Hewlett Packard LCR meter.

III. RESULTS

A. X-ray photoelectron spectroscopy (XPS)

Following the CVC process the O and C signals at the surface were reduced below the detection limit of the XPS, which is approximately 0.3 at. %.⁴⁴ The Ga 3*d* and N 1*s* core level photoelectron peaks obtained from the CVC treated surfaces were fit with single peaks located at 20.4 ± 0.1 eV [full width at half maximum (FWHM) = 1.3 eV] and 398.0 ± 0.1 eV (FWHM = 1.2 eV), respectively. The peak positions were consistent from one film to the next as evidenced by the plot in Fig. 2. The Ga/N ratio on the clean surfaces, determined from the peak areas of the Ga 3*d* and N 1*s* core levels and corresponding sensitivity factors (Ga 3*d*, 0.310 and N 1*s*, 0.420), was calculated to be ~ 1.03 for all films used in this study.

Changes in the band bending at the surface with subsequent metal depositions were monitored using the Ga 3*d* core level. Figure 1(a) shows progressive shifts to lower binding energies to a total of 0.8 eV with sequential Pt deposition through 0.5 nm. Similar spectra for Au and Ag (not shown) indicate total shifts of 0.5 and 0.2 eV, respectively, towards lower binding energies after depositing a total of 0.5 nm Au and 1 nm Ag. The as-deposited Pt, Au, and Ag/GaN interfaces were abrupt, unreacted, and epitaxial as evidenced by the constant value of the FWHM of the Ga 3*d* core level spectra throughout each deposition and as revealed by high-resolution transmission electron microscopy and electron dif-

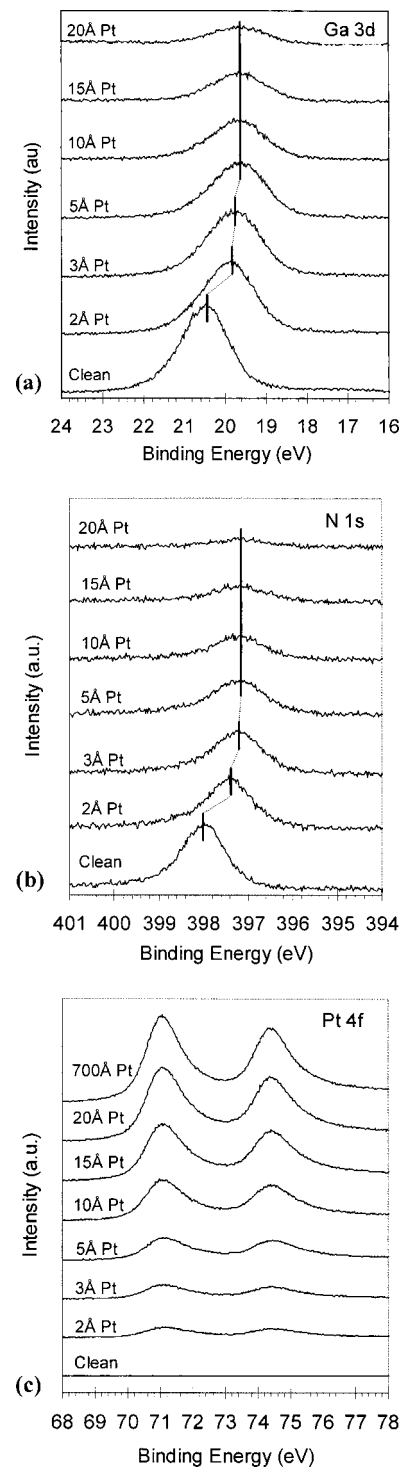


FIG. 1. XPS (a) Ga 3*d* (b) N 1*s*, and (c) Pt 4*f* core level photoelectron peaks as a function of the thickness of a Pt film deposited on a chemical vapor cleaned *n*-GaN surface. All spectra were acquired using Mg *K* α ($h\nu = 1253.6$ eV) radiation.

fraction of the interfaces.³⁵ Subsequent Pt, Au, and Ag depositions in excess of the thicknesses noted above did not result in additional shifts in the Ga 3*d* peak energy. These shifts in peak energy are assumed to reflect a 1:1 correspondence with changes in the band bending at the surface. The direction of the core level shifts is consistent with that expected for large work function metals on *n*-type GaN wherein the

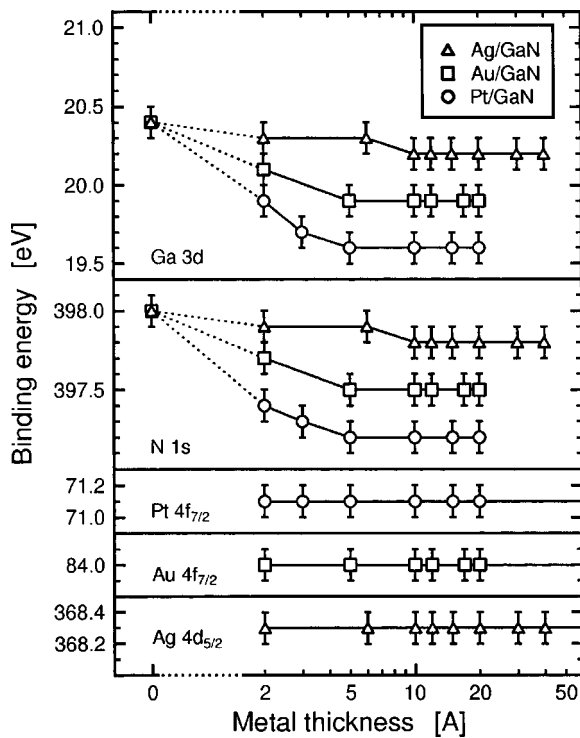


FIG. 2. Positions of the Ga 3*d*, N 1*s*, Pt 4*f*, Au 4*f*, and Ag 4*d* XPS core level photoelectron peaks acquired for different thicknesses of Pt, Au, and Ag, respectively.

shifts are toward lower binding energy (i.e., the bands bend upward towards the surface). The magnitudes and the directions of the shifts in the N 1*s* core level with sequential Pt, Au, and Ag depositions are equivalent to those for the Ga 3*d*, as shown by example in Fig. 1(b) for the sequential deposition of Pt. The latter results provide additional evidence in support of the interpretation of the observed shifts as changes in band bending rather than chemically induced shifts

The 4*f* doublet structures for Pt and Au (4*f*_{7/2} and 4*f*_{5/2}) as well as the 4*d* doublet structures for Ag (4*d*_{5/2} and 4*d*_{3/2}) did not shift with increasing metal thickness, as illustrated in Fig. 1(c) for Pt. They are located at 71.1±0.1 and 74.4±0.1 eV, 84.0±0.1 and 87.7±0.1 eV, and 368.3±0.1 and 374.3±0.1 eV for Pt, Au, and Ag, respectively. The separation of these peaks is consistent with those measured for bulk metals.^{44,45} Moreover, the FWHM values of 1.2 eV for Pt and 1.0 eV for Au and Ag did not change with the metal thickness. The photoelectron peak positions of all the spectral lines discussed above are summarized in Fig. 2.

Schottky barrier heights (SBH) were determined from the XPS data using the relation shown in Eq. (1). This equation was previously employed by Waldrop and Grant^{46,47} for the calculation of the SBH of metals on SiC and GaAs.

$$\phi_B = E_g - E_{\text{VBM}}^i + (E_{\text{core}}^i - E_{\text{core}}^m), \quad (1)$$

E_g is the band gap, E_{core}^m is the binding energy of the semiconductor core level peak following metal deposition, E_{core}^i is the initial binding energy of the core level peak, and E_{VBM}^i is the binding energy of the valence band maximum (VBM) of the semiconductor. All binding energies are measured relative to the Fermi energy. An advantage of this approach

is that since it is based on differences in core level energies, the result is not sensitive to small calibration variations. Using $E_g = 3.4$ eV, $E_{\text{VBM}}^i = 3.0$ eV from the UPS measurements presented below and the core level shifts $E_{\text{core}}^i - E_{\text{core}}^m$ from the XPS measurements, Eq. (1) results in $\phi_B^{\text{Pt}} = 1.2 \pm 0.1$ eV, $\phi_B^{\text{Au}} = 0.9 \pm 0.1$ eV, and $\phi_B^{\text{Ag}} = 0.6 \pm 0.1$ eV. Note that identical values are obtained for either the Ga or N core levels.

B. Ultraviolet photoelectron spectroscopy (UPS)

Figures 3(a)–3(c) show the evolution of the respective UPS valence band spectra with sequential Pt, Au, and Ag depositions. Assuming an electron effective mass, carrier concentration, and a room temperature band gap of $0.20m_0$, $1.0 \times 10^{17} \text{ cm}^{-3}$, and 3.4 eV,⁴⁸ respectively, the position of the VBM is predicted to be 3.3 eV below the Fermi level. A linear fit of the high kinetic energy side of the spectrum indicates that the VBM on the clean *n*-GaN surface is located 3.0 ± 0.1 eV below the Fermi level ($E_F = 0$ eV). Therefore the upward band bending and the electron affinity at the clean surface were calculated to be 0.3 ± 0.1 and 3.1 ± 0.2 eV, respectively.

The bulk GaN feature located at -13.4 ± 0.1 eV exhibited a pronounced shift to lower binding energies with sequential Pt, Au, and Ag depositions. Maximum shifts of 0.8 ± 0.1 and 0.5 ± 0.1 eV were achieved for 0.5 nm thick Pt and Au films, respectively; a 0.2 ± 0.1 eV shift was observed for a total Ag thickness of 0.2 nm. Subsequent shifts with additional metal deposition could not be observed due to the attenuation in the intensity of the bulk feature. The agreement between the magnitude and direction of the shifts observed for the bulk feature in the valence band spectra and those observed for both the Ga 3*d* and N 1*s* core level spectra suggest that the bulk feature itself may be a core level peak associated with Ga and/or N.

The high kinetic energy side of the valence band spectra for sequential Pt, Au, and Ag depositions is magnified in Figs. 4(a)–4(c), respectively. The leading edge in each spectrum is shifted towards the Fermi level with increasing metal thickness. Fermi level emission is observed for 1.0, 0.5, and 0.2 nm thick Pt, Au, and Ag films, respectively, which subsequently marks the onset of the metallic properties of the thin films. Figure 4(b) also shows a feature marked by S_1 for the thicker Au layers which corresponds to a known surface state at the Au(111) surface.^{49,50} The UPS valence band spectra may also be employed to determine the Schottky barrier height using Eq. (2).

$$\phi_B = E_g - (E_f - E_{\text{VBM}}^m), \quad (2)$$

E_{VBM}^m is the position of the VBM at the onset of electronic equilibrium, wherein the leading edge no longer shifts with additional metal deposition.⁵⁰ The direct determination of E_{VBM}^m is very often difficult, as the metallic features tend to dominate in the high kinetic energy region of the spectrum and cover the signal from the VBM. Figures 3(a)–3(c) clearly show that the metal *d*-band signals located at -5 to 0 eV, -8 to -5 eV, and -8 to -4 eV for Pt, Au, and Ag, respectively, are the most prominent features in the spectra.

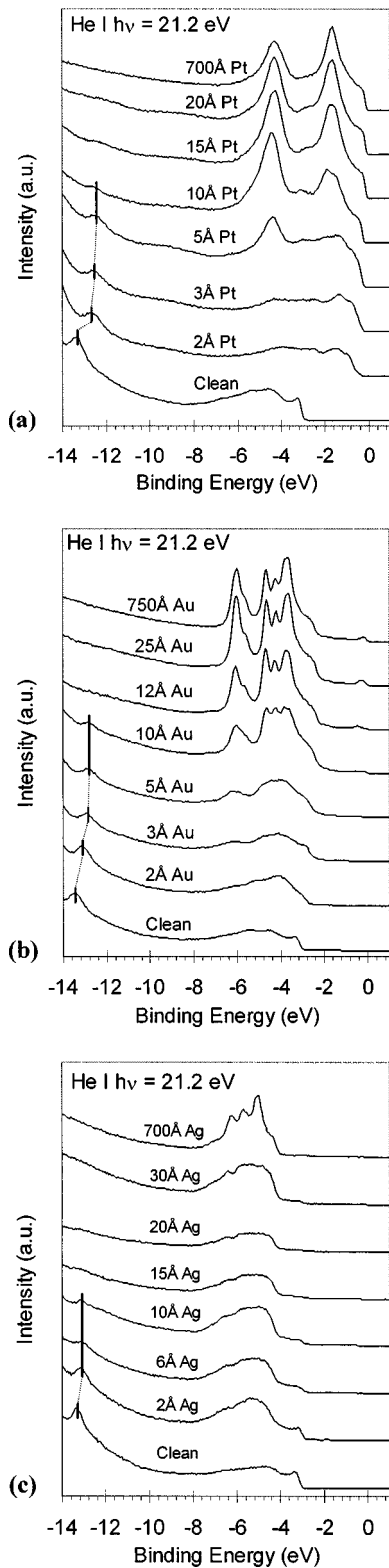


FIG. 3. UPS valence band spectra from the *n*-GaN surface following both chemical vapor cleaning and sequential (a) Pt, (b) Au, and (c) Ag metallization. The band bending is induced by the deposition of all three metals and is indicated by the movement of the core level feature located at ~ -13 eV. All spectra were acquired using the He I photon line ($h\nu = 21.2$ eV). The binding energy is measured with respect to the Fermi level ($E_F = 0$ eV).

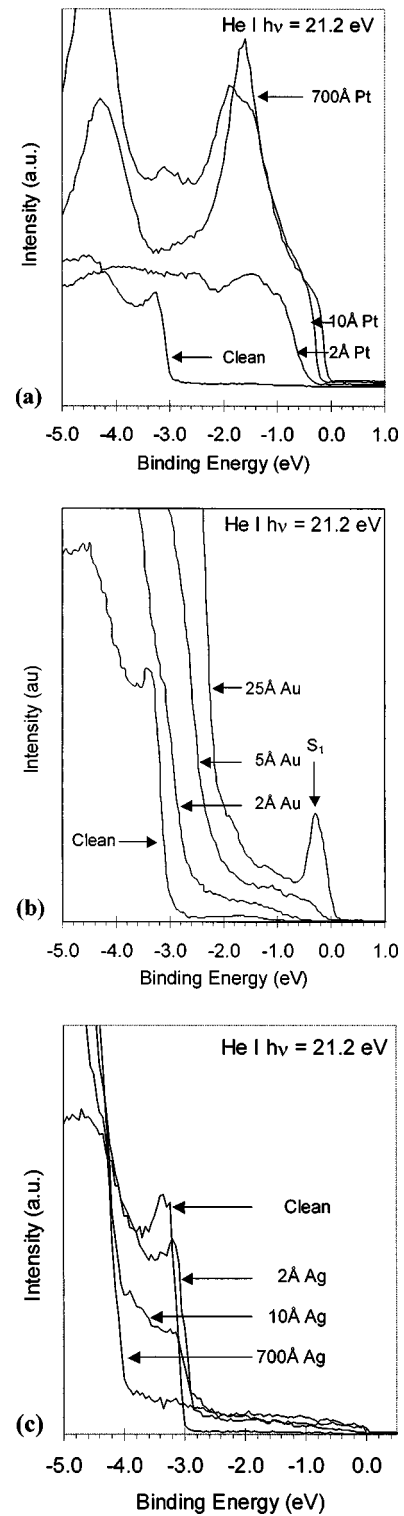


FIG. 4. (a) – (c) Expanded view of the high kinetic energy region for Figs. 3(a)–3(c), respectively.

In this case the E_{VBM}^m could only be observed for thin Ag films, as the Ag signal was not very intense in the -4 to 0 eV range. For the Pt and Au cases the shift in the bulk GaN feature located at $\sim 13.4 \pm 0.1$ eV was observed to metal thicknesses as large as 1.0 nm; it was used as a reference, since the peak position relative to the VBM remained con-

stant. Therefore E_{VBM}^m can be calculated according to Eq. (3) below where ΔE_{bulk} is the maximum shift in bulk feature with respect to the initial

$$E_{\text{VBM}}^m = E_{\text{VBM}}^i + \Delta E_{\text{bulk}} \quad (3)$$

position on the clean surface. Note that this procedure was tested for the case of Ag wherein the shifts in the bulk feature were found to be equivalent to those observed for the VBM shown in Figs. 3(c) and 4(c), respectively. The Schottky barriers calculated according to Eqs. (2) and (3) were 1.2 ± 0.1 , 0.9 ± 0.1 , and 0.6 ± 0.1 eV for Pt, Au, and Ag, respectively.

The work function of the metals can be determined using the following expression:

$$\phi_m = h\nu - W, \quad (4)$$

where $h\nu$ is the energy of the incident photons (21.2 eV) and W is the width of the spectrum. The latter values were determined to be 15.5 ± 0.1 , 15.9 ± 0.1 , and 16.8 ± 0.1 eV for Pt, Au, and Ag, respectively. This results in work functions of 5.7 ± 0.2 , 5.3 ± 0.2 , and 4.4 ± 0.2 eV for Pt, Au, and Ag, respectively.

C. Electrical measurements

Representative semilogarithmic plots of the $I-V$ data for the Pt, Au, and Ag contacts are shown in Fig. 5(a). All contacts exhibited rectifying behavior. The leakage currents at -10 V bias were less than 1 nA, 90 nA, and 0.8 mA for the Pt, Au, and Ag contacts, respectively. The breakdown was “soft” for all contacts with leakage currents increasing under reverse bias by a factor of ~ 10 per 10 V for Pt and Au and a factor of 2 to 3 per 10 V for Ag. Catastrophic breakdown occurred between -80 and -75 V, -60 and -50 V, and -50 and -40 V for the Pt, Au, and Ag contacts, respectively. Subsequent measurements revealed that the contact structures were no longer rectifying, with nonlinear symmetric current flow being observed for both forward and reverse bias.

The $I-V$ characteristics for all contacts studied were modeled using Eqs. (5) and (6) below, which are consistent with thermionic emission theory.

$$I = I_o \cdot \left(\exp \left[\frac{qV - IR_s}{nkT} \right] - 1 \right), \quad (5)$$

$$I_o = A \cdot A^{**} T^2 \cdot e^{-q \cdot \phi_b / kT} \quad (6)$$

A is the contact area, A^{**} is the effective Richardson constant, q is the electronic charge, n is the ideality factor, k is Boltzman’s constant, T is the temperature, and ϕ_b is the Schottky barrier height. If one assumes a negligible series resistance and that $V > 3kT/q$, a plot $\ln(I)$ versus V should reveal a linear region which extends over at least two decades of current. The Schottky barrier height and ideality factor are calculated from the x intercept and slope, respectively. Expanded views of the plots of the $I-V$ data presented in Fig. 5(a) are shown in Fig. 5(b) over the range from 0 to 1.2 V. Linear regions occur from 0.5 to 0.9 V, 0.1 to 0.5 V, and 0.1 to 0.2 V for the Pt, Au, and Ag contacts, respectively. This corresponds to a current range of over 5 decades

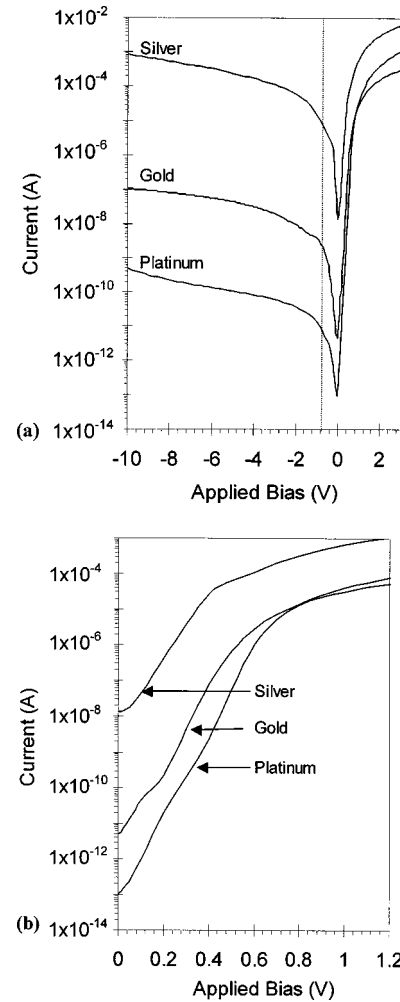


FIG. 5. (a) Semilogarithmic plot of the current–voltage ($I-V$) characteristics for Pt, Au, and Ag Schottky contacts on chemical vapor cleaned n -GaN. (b) Expanded view of the forward current region in (a).

for Pt and Au and approximately 2 decades for Ag. The deviation at higher voltages is due to the series resistance of the GaN film. Extrapolating the linear region to the ordinate provided Schottky barrier heights of 1.15 ± 0.01 eV, 0.87 ± 0.01 eV, and 0.58 ± 0.01 eV for Pt, Au, and Ag, respectively. The theoretical value for the effective Richardson constant²³ ($26.4 \text{ A cm}^{-2} \text{ K}^{-2}$) is assumed in calculating the Schottky barrier heights. The slopes of these regions resulted in respective ideality factors of 1.14 ± 0.01 , 1.13 ± 0.01 , and 1.20 ± 0.1 for the Pt, Au, and Ag contacts.

The $C-V$ data for Pt and Au contacts are shown in Fig. 6. The capacitance of a metal–semiconductor junction as a function of voltage is described by Eq. (7), where A is the contact area, V_{bi} is the built-in voltage, V is the applied voltage, N_d is the donor concentration, ϵ_{sc} is the dielectric constant of the semiconductor, and k , T , ϵ_o , and q have their usual definitions.

$$\frac{A^2}{C^2} = \frac{2 \cdot \left(V_{\text{bi}} - V - \frac{kT}{q} \right)}{q \epsilon_{\text{sc}} \cdot \epsilon_o \cdot N_d}. \quad (7)$$

The carrier concentration may be extracted from the slope of

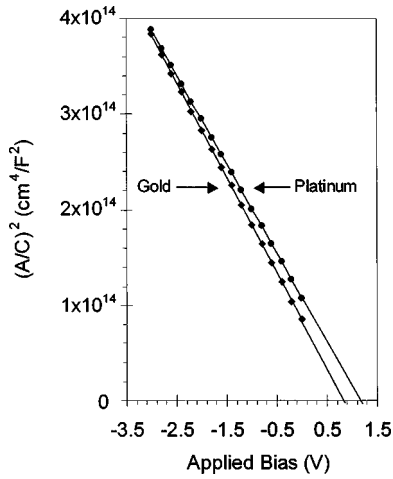


FIG. 6. Capacitance–voltage ($C-V$) characteristics for Pt and Au Schottky contacts on chemical vapor cleaned n -GaN. The ordinate is the square of the ratio of the contact area (A) and the capacitance (C).

a plot of A^2/C^2 versus V . The intercept on the voltage axis provides a quantitative measure of the Schottky barrier height according to Eq. (8).

$$\phi_B = V_i + V_o + \frac{kT}{q}, \quad (8)$$

V_i is the intercept on the voltage axis, V_o is the difference between the conduction band minimum and the Fermi level, and k , T , and q have their usual definitions. The slopes in Fig. 6 were measured to be -9.3×10^{13} and $-9.9 \times 10^{13} \text{ cm}^4/\text{F}^2/\text{V}$ for Pt and Au, respectively. This corresponds to a net impurity concentration in the GaN of $1.6 \times 10^{17} \text{ cm}^{-3}$ assuming that the dielectric constant of this material is 9.0. The intercepts were 1.16 and 0.86 V for Pt and Au, respectively. This corresponds to Schottky barrier heights of 1.24 ± 0.1 eV and 0.96 ± 0.1 eV for Pt and Au, respectively. $C-V$ measurements were not made on the Ag/ n -GaN Schottky contact structures. The values for each Schottky barrier height and the corresponding technique from which the initial data were acquired are shown in Table II.

IV. DISCUSSION

Pt, Au, and Ag formed an abrupt, unreacted metal–semiconductor interface, as evidenced by the constant full width at half maximum (FWHM) for the Ga $3d$ photoelectron peak with sequential metal deposition. The absence of additional peaks in the Ga $3d$, N $1s$, and the corresponding metal spectra, indicating the formation of alloys, lends further support to this conclusion. These results agree with those from a previous study by Wu *et al.*²⁰ that investigated

TABLE III. Summary of experimentally determined values for Pt on GaN(0001).

| Pt/GaN (0001) | This work | Literature |
|--------------------------------------|-----------------|----------------------------|
| Schottky barrier height [eV] : XPS | 1.2 ± 0.1 | 1.65 (Ref. 20) |
| Schottky barrier height [eV] : UPS | 1.2 ± 0.1 | NR |
| Schottky barrier height [eV] : $I-V$ | 1.15 ± 0.01 | 0.88–1.13 (Refs. 11–19) |
| Schottky barrier height [eV] : $C-V$ | 1.24 ± 0.05 | 0.91–1.27 (Refs. 11–19) |
| Metal work function [eV] | 5.7 ± 0.1 | NR |
| Ideality factor | 1.14 ± 0.01 | 1.002–1.7 (Refs. 11–19) |

NR=not reported.

Pt and Au contacts deposited on n -GaN surfaces previously treated using an ISA process. Sporken *et al.*²⁹ investigated Pt/ n -GaN and Au/ n -GaN interfaces via depth profiling XPS and observed an interface that was significantly more diffuse. However, an *in situ* investigation from the same study did not reveal any interdiffusion or reaction at the contact interface and attributed the diffuse quality of the depth profiles to large differences in the sputtering yields for Pt, Au, and GaN. There were also significant amounts of both C and O contamination at the interface, which would preclude the formation of an abrupt metal–semiconductor interface.

The experimentally determined values for the barrier heights and ideality factors obtained in this work as well as those reported in the literature are summarized in Tables II–V. It should be emphasized that the different techniques employed in the present research show consistent results in terms of the calculated values of the SBHs. The *ex situ* and *in situ* measurements agree to within the calculated experimental error for each metal studied. However, the $C-V$ measurements resulted in consistently larger barrier heights compared to those obtained using the $I-V$ technique. Good agreement with SBHs reported in the literature is found for the results of $I-V$ and $C-V$ measurements but deviations are found for the photoelectron emission experiments.

The ideality factors reported for the three metals are in general agreement with our values. This is also nearly true for the breakdown voltages for Pt and Au. However, the reported values of the leakage currents under reverse bias range over several orders of magnitude. The cause of this spread is not clear; however, it is likely due to the preparation of the interface as well as the bulk material. For instance, films grown by different techniques and/or on different substrates can have different microstructures, surface terminations, polarities, defect densities, and bulk densities. Therefore care must be taken when comparing device parameters from various samples.

TABLE II. Summary of Schottky barrier heights and corresponding experimental technique.

| Contact | Metal work function (Φ) | $\Phi_b I-V$ (eV) | Ideality factor (n) | $\Phi_b C-V$ (eV) | Φ_b XPS (eV) | Φ_b UPS (eV) | leakage at -10 V (A) |
|---------|--------------------------------|-------------------|-------------------------|-------------------|-------------------|-------------------|------------------------|
| Pt | 5.7 ± 0.1 | 1.15 ± 0.01 | 1.14 ± 0.01 | 1.24 ± 0.05 | 1.2 ± 0.1 | 1.2 ± 0.1 | 1×10^{-9} |
| Au | 5.3 ± 0.1 | 0.87 ± 0.01 | 1.13 ± 0.01 | 0.96 ± 0.05 | 0.9 ± 0.1 | 0.9 ± 0.1 | 9×10^{-8} |
| Ag | 4.4 ± 0.1 | 0.58 ± 0.01 | 1.20 ± 0.01 | NR | 0.6 ± 0.1 | 0.6 ± 0.1 | 8×10^{-4} |

TABLE IV. Summary of experimentally determined values for Au on GaN(0001).

| Au/GaN (0001) | This work | Literature |
|--|-----------|-------------------------------------|
| Schottky barrier height [eV] : XPS | 0.9±0.1 | 1.15–1.3 (Refs. 20 and 29) |
| Schottky barrier height [eV] : UPS | 0.9±0.1 | NR |
| Schottky barrier height [eV] : <i>I</i> – <i>V</i> | 0.87±0.01 | 0.8–1.88 (Refs. 12,13,21–28,30,33) |
| Schottky barrier height [eV] : <i>C</i> – <i>V</i> | 0.96±0.05 | 0.94–1.16 (Refs. 12,13,21–27,33) |
| Metal work function [eV] | 5.3±0.1 | NR |
| Ideality factor | 1.13±0.01 | 1.03–4 (Refs. 12,13,21–26,28,30,33) |

NR=not reported.

The predicted Schottky barrier height is now considered based on the electron affinity obtained in this study and Eq. (9), which is consistent with the Schottky–Mott model.

$$\phi_{Bn} = \phi_m - \chi_{sc} \tag{9}$$

Substituting the experimentally determined values for the metal work functions resulted in Schottky barrier heights of 2.6, 2.2, and 1.3 eV for Pt, Au, and Ag, respectively. The fact that these values are significantly larger than those determined from the experimental data (XPS, UPS, and *I*–*V*) presented above suggests that there is an additional interface dipole that results in a reduction of the Schottky barrier by 1.4, 1.3, and 0.7 eV for Pt, Au, and Ag, respectively.

Figure 7 shows the dependence of the Schottky barrier height on the work function of the contact metal. The Schottky–Mott model predicts a 1:1 correspondence between changes in the Schottky barrier height and an increasing or a decreasing metal work function and is subsequently shown with a slope of 1. The slope of the line determined from this research is ~0.44 which suggests that although the Schottky barrier height shows some dependence on the metal work function there is a significant contribution from both extrinsic and intrinsic surface states as well as metal induced gap states (MIGS). The complex interaction between each of these contributions is manifest in the interface dipole term.

Wu *et al.*²⁰ investigated the electrical and chemical properties of Al, Ti, Mg, Au, and Pt metals deposited on *n*-GaN surfaces previously treated using an ISA technique. The elec-

TABLE V. Summary of experimentally determined values for Ag on GaN(0001)

| Ag/GaN (0001) | This work | Literature |
|--|-----------|-----------------------------|
| Schottky barrier height [eV] : XPS | 0.6±0.1 | 0.7 (Ref. 30) |
| Schottky barrier height [eV] : UPS | 0.6±0.1 | NR |
| Schottky barrier height [eV] : <i>I</i> – <i>V</i> | 0.58±0.01 | 0.54–0.89 (Refs. 13,31–33) |
| Schottky barrier height [eV] : <i>C</i> – <i>V</i> | NR | 0.66–1.61 (Refs. 13 and 33) |
| Metal work function [eV] | 4.4±0.1 | NR |
| Ideality factor | 1.20±0.01 | 1.24–1.6 (Refs. 13,31–33) |

NR=not reported.

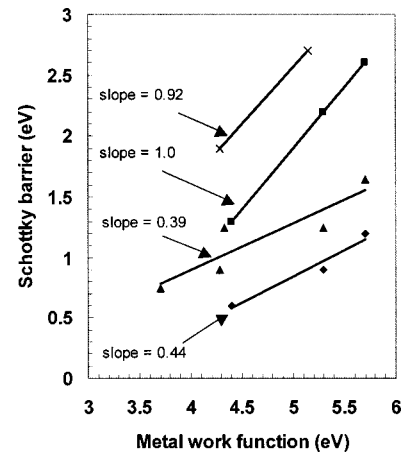


FIG. 7. Work function dependence of the Schottky barrier height (SBH) for metal contacts on *n*-GaN. The slope is calculated for data taken from this work (◆), Wu *et al.*(Ref. 20)(▲), Bermudez *et al.*(Ref. 38)(×), and the Schottky–Mott model (■).

tron affinity and upward band bending at the clean *n*-GaN surface were 3.5 and 0.75 eV, respectively. Assuming that the Al, Ti, Mg, Pt, and Au work functions are 4.28, 4.33, 3.7, 5.7, and 5.3 eV, respectively, the interface dipole contributions were calculated to be 0.15, 0.42, 0.55, 0.55, and 0.55 eV for Al, Ti, Mg, Pt, and Au, respectively. In this case the slope of the line was calculated to be ~0.39. Although the slope is approximately the same as that found in the present research, the interface dipole contributions to the Schottky barrier heights for Au and Pt are significantly smaller. This difference may be attributed to the effects of the ISA surface preparation process as evidenced by the fact that the values for the electron affinity and band bending at the prepared surface are significantly larger than those from the present work. As the Schottky barriers were determined using photoemission measurements alone, the observed differences as compared to the present research may also be attributed to small differences in equipment calibration.

Bermudez *et al.*³⁸ investigated the electrical and chemical properties of Al and Ni metals deposited on *n*-GaN surfaces previously treated using a Ga deposition and desorption technique. The electron affinity and upward band bending at the clean *n*-GaN surface were 2.7±0.3 and 1.4 eV, respectively. Assuming that the Al and Ni work functions are 4.28 and 5.15 eV, respectively, the interface dipole contributions were calculated to be 0.32 and 0.25 eV for Al and Ni, respectively. In this case the slope of the line was calculated to be ~0.92. The effects of the surface preparation technique are again manifest in the difference between the interface dipole contribution measured for Al by Bermudez and that found in the study by Wu *et al.*²⁰ In this case the dependence of the Schottky barrier height on the metal work function is the strongest that has been reported to date and closely approaches the Schottky–Mott limit.

For each of the studies above the differences in the interface dipole contribution for different metals deposited on identically prepared surfaces may be attributed to the contributions from MIGS. The effects of MIGS has been thoroughly investigated by Kampen *et al.*³² However, the effects

of the surface preparation technique and the subsequent contribution to the interface dipole term appear to have the greatest effect on both the Schottky barrier heights of individual metals as well as the overall dependence of the Schottky barrier height on the work function of the metal.

V. SUMMARY

Clean and ordered *n*-type GaN(0001) surfaces were used to investigate both the chemical and the electrical properties of Pt, Au, and Ag Schottky contacts. The electron affinity and upward band bending at the clean *n*-GaN surface were 3.1 ± 0.1 eV and 0.3 ± 0.1 eV, respectively. These three metals formed abrupt and unreacted metal–semiconductor interfaces. The Schottky barrier heights determined from the data acquired using XPS, UPS, $I-V$, and $C-V$ techniques all agreed to within the experimental error for each contact metal and had the values of 1.2 ± 0.1 , 0.9 ± 0.1 , and 0.6 ± 0.1 eV for Pt, Au, and Ag, respectively. Although the Schottky barrier heights showed a dependence on the metal work function, there were significant contributions from MIGS, as well as both extrinsic and intrinsic surface states. The sum of these additional effects are manifest in the interface dipole contributions to the Schottky barrier height which were measured to be ~ 1.4 , 1.3 , and 0.7 eV for Pt, Au, and Ag, respectively.

ACKNOWLEDGMENTS

Cree, Inc. provided the Si-doped GaN(0001) films on 6H–SiC(0001) wafers used in this study. The authors also acknowledge the support of the Office of Naval Research via Contracts No. N00014-98-1-0654 (John Zolper and Harry Dietrich, Monitors) and No. N00014-99-1-0729 (Colin Wood, Monitor). R.F.D. was partially supported by the Kobe Steel, Ltd. University Professorship.

- ¹S. Nakamura, M. Senoh, N. Iwasa, and S. Nagahama, *Jpn. J. Appl. Phys.*, Part 2 **34**, L797 (1995).
- ²S. Yoshida and J. Suzuki, *Jpn. J. Appl. Phys.*, Part 2 **38**, L851 (1999).
- ³B. S. Shelton, D. J. H. Lambert, J. J. Huang, M. M. Wong, U. Chowdhury, T. G. Zhu, H. K. Kwon, Z. Liliental-Weber, M. Benaroma, M. Feng, and R. S. Dupuis, *IEEE Trans. Electron Devices* **48**, 490 (2001).
- ⁴N. Stath, V. Harle, and J. Wagner, *Mater. Sci. Eng.*, B **80**, 224 (2001).
- ⁵S. C. Binari, K. Doverspike, G. Kelner, H. B. Dietrich, and A. E. Wickenden, *Solid-State Electron.* **41**, 177 (1997).
- ⁶T. Egawa, K. Nakamura, H. Ishikawa, T. Jimbo, and M. Umeno, *Jpn. J. Appl. Phys.*, Part 1 **38**, 2630 (1999).
- ⁷M. A. Kahn, J. N. Kuznia, A. R. Bhattarai, and D. T. Olsen, *Appl. Phys. Lett.* **62**, 1786 (1993).
- ⁸Y.-K. Su, Y.-Z. Chiou, F.-S. Juang, S.-J. Chang, and J.-K. Sheu, *Jpn. J. Appl. Phys.*, Part 1 **40**, 2996 (2001).
- ⁹W. Gu, S. J. Chua, X. H. Zhang, M. S. Hao, J. Zhang, W. Wang, and W. Liu, *Phys. Status Solidi A* **188**, 329 (2001).
- ¹⁰M. A. Kahn, J. N. Kuznia, D. T. Olsen, M. Blasingame, and A. R. Bhattarai, *Appl. Phys. Lett.* **63**, 2455 (1993).
- ¹¹Q. Z. Liu, K. V. Smith, E. T. Yu, S. S. Lau, N. R. Perkins, and T. F. Kuech, *On the Epitaxy of Metal Films on GaN* (Materials Research Society, Pittsburgh, PA, 1997), Vol XXV+1251.
- ¹²A. C. Schmitz, A. T. Ping, M. A. Kahn, Q. Chen, J. W. Yang, and I. Adesida, *Semicond. Sci. Technol.* **11**, 1464 (1996).
- ¹³A. C. Schmitz, A. T. Ping, M. A. Kahn, Q. Chen, J. W. Yang, and I. Adesida, *J. Electron. Mater.* **27**, 255 (1998).
- ¹⁴Z. Fan, M. W. Kim, A. E. Botcharev, K. Suzue, H. Morkoc, K. Duxstad, and E. E. haller, *J. Electron. Mater.* **25**, 1703 (1996).
- ¹⁵K. Suzue, S. N. Mohammad, Z. F. Fan, W. Kim, O. Aktas, A. E. Botcharev, and H. Morkoc, *J. Appl. Phys.* **80**, 4467 (1996).
- ¹⁶S. N. Mohammad, Z. Fan, A. E. Botcharev, W. Kim, O. Aktas, A. Salvador, and H. Morkoc, *Electron. Lett.* **32**, 598 (1996).
- ¹⁷L. Wang, M. I. Nathan, T. H. Lim, M. A. Kahn, and Q. Chen, *Appl. Phys. Lett.* **68**, 1267 (1996).
- ¹⁸J. D. Guo, M. S. Feng, R. J. Guo, F. M. Pan, and C. Y. Chang, *Appl. Phys. Lett.* **67**, 2657 (1995).
- ¹⁹Q. Z. Liu, L. S. Yu, S. S. Lau, J. M. Redwing, N. R. Perkins, and T. F. Kuech, *Appl. Phys. Lett.* **70**, 1275 (1997).
- ²⁰C. I. Wu and A. Kahn, *J. Vac. Sci. Technol. B* **16**, 2218 (1998).
- ²¹E. V. Kalinina, N. I. Kuznetsov, V. A. Dmitriev, K. G. Irvine, and C. H. Carter, Jr., *J. Electron. Mater.* **25**, 831 (1996).
- ²²E. V. Kalinina, N. I. Kuznetsov, A. I. Babanin, V. A. Dmitriev, and A. V. Shchukarev, *Diamond Relat. Mater.* **6**, 1528 (1997).
- ²³P. Hacke, T. Detchprohm, K. Hiramatsu, and N. Sawaki, *Appl. Phys. Lett.* **63**, 2676 (1993).
- ²⁴M. Sawada, T. Sawada, Y. Yamagata, K. Imai, H. Kimura, M. Yoshino, K. Iizuka, and H. Tomozawa, *J. Cryst. Growth* **189**, 706 (1998).
- ²⁵M. R. H. Kahn, T. Detchprohm, P. Hacke, K. Hiramatsu, and N. Sawaki, *J. Phys. D* **28**, 1169 (1995).
- ²⁶Y. Kribes, I. Harrison, B. Tuck, T. S. Cheng, and C. T. Foxon, *Semicond. Sci. Technol.* **12**, 913 (1997).
- ²⁷S. C. Binari, H. B. Dietrich, G. Kelner, L. B. Rowland, K. Doverspike, and D. K. Gaskill, *Electron. Lett.* **30**, 909 (1994).
- ²⁸Z. Z. Bandic, P. M. Bridger, E. C. Piquette, T. C. McGill, R. P. Vaudo, V. M. Phanse, and J. M. Redwing, *Appl. Phys. Lett.* **74**, 1266 (1999).
- ²⁹R. Sporcken, C. Silien, F. Malengreau, K. Grigorov, R. Caudano, F. J. Sanchez, E. Calleja, E. Munoz, B. Beaumont, and P. Gibart, *MRS Internet J. Nitride Semicond. Res.* **2**, 23 (1997).
- ³⁰L. He, X. J. Wang, and R. Zhang, *J. Vac. Sci. Technol. A* **17**, 1217 (1999).
- ³¹T. G. G. Maffei, S. A. Clark, P. R. Dunstan, S. P. Wilks, D. A. Evans, F. Peiro, H. Riechert, and P. J. Parbrook, *Phys. Status Solidi A* **176**, 751 (1999).
- ³²T. U. Kampen and W. Monch, *Appl. Surf. Sci.* **117/118**, 388 (1997).
- ³³S. Arulkumaran, T. Egawa, G. Y. Zhao, H. Ishikawa, T. Jimbo, and M. Umeno, *Jpn. J. Appl. Phys.*, Part 2 **39**, L351 (2000).
- ³⁴S. Miller and P. H. Holloway, *J. Electron. Mater.* **25**, 1709 (1996).
- ³⁵E. A. Preble, K. M. Tracy, S. Kiesel, H. McLean, P. Q. Miraglia, R. J. Nemanich, M. Albrecht, D. J. Smith, and R. F. Davis, *J. Appl. Phys.* **91**, 2133 (2002).
- ³⁶D. K. Schroder, *Semiconductor Material and Device Characterization* (Wiley, New York, 1998), p. 156.
- ³⁷R. T. Tung, in *Contacts to Semiconductors*, edited by L. J. Brillson (Noyes, New Jersey, 1993), Chap. 3.
- ³⁸V. M. Bermudez, T. M. Jung, K. Doverspike, and A. E. Wickenden, *J. Appl. Phys.* **79**, 110 (1996).
- ³⁹M. Eyckeler, W. Monch, T. U. Kampen, R. Dimitrov, O. Ambacher, and M. Stutzman, *J. Vac. Sci. Technol. B* **16**, 2224 (1998).
- ⁴⁰D.-W. Kim, J. C. Bae, W. J. Kim, H. K. Baik, J.-M. Myoung, and S.-M. Lee, *J. Electron. Mater.* **30**, 183 (2001).
- ⁴¹A. R. Smith, R. M. Feenstra, D. W. Greve, M.-S. Shin, M. Skowronski, J. Neugebauer, and J. E. Northrup, *Appl. Phys. Lett.* **72**, 2114 (1998).
- ⁴²S. W. King, J. P. Barnak, M. D. Bremser, K. M. Tracy, C. Ronning, R. F. Davis, and R. J. Nemanich, *J. Appl. Phys.* **84**, 5248 (1998).
- ⁴³D. A. Shirley, *Phys. Rev. B* **5**, 4709 (1972).
- ⁴⁴D. Briggs and M. P. Seah, *Practical Surface Analysis Volume 1* (Wiley, West Sussex, 1983).
- ⁴⁵J. F. Moulder, W. M. F. Stickel, P. R. E. Sobol, and K. D. H. Bomben, *Handbook of X-ray Photoelectron Spectroscopy, 1st ed.* (Perkin Elmer, Physical Electronics Division, 1992).
- ⁴⁶J. R. Waldrop and R. W. Grant, *Appl. Phys. Lett.* **52**, 1794 (1988).
- ⁴⁷J. R. Waldrop and R. W. Grant, *Appl. Phys. Lett.* **62**, 2685 (1993).
- ⁴⁸S. Strite and H. Morkoc, *J. Vac. Sci. Technol. B* **10**, 1237 (1992).
- ⁴⁹C. M. Whelan, C. J. Barnes, C. G. H. Walker, and N. M. D. Brown, *Surf. Sci.* **425**, 195 (1999).
- ⁵⁰J. Van der Weide and R. J. Nemanich, *J. Vac. Sci. Technol. B* **10**, 1940 (1992).